

# In-Field Hall Probe Mapping System for Characterization of YBCO Weldings

S. Iliescu, S. Sena, X. Granados, E. Bartolomé, T. Puig, X. Obradors, M. Carrera, J. Amorós, S. Krakunovska and T. Habisreuther

**Abstract**—Artificial welding of melt-textured YBCO blocks opens the door to the fabrication of large, complex-shaped pieces required for applications. In order to evaluate the superconducting quality of the welds, we have developed a Hall probe mapping system, able to record the local magnetization at 77 K under dynamic applied fields in the range of  $-1$  to  $1$  T. The system was used to characterize welded samples prepared with a new Ag induced surface melting joining technique. The magnetization maps of unwelded and welded samples of various qualities are compared and discussed. The current distributions associated to the Hall maps were calculated using the Caragol software. The magnetization and current distribution maps over the joint show that good quality welds can be reached with this joining method.

**Index Terms**—Welding YBCO; Hall probe; magnetization; critical current.

## I. INTRODUCTION

THE application of melt-textured  $\text{YBa}_2\text{Cu}_3\text{O}_7$  in engineering devices, such as rotors and magnetic bearings for superconducting motors or current limiters, requires mastering the production of large size, complex-shaped pieces. Artificial welding of separate YBCO grains, grown by the Top-Seeding technique, provides a way to obtain such objects. Different joining techniques have been proposed, based on the use of low-melting point welding agents like REBCO oxides ( $\text{RE}=\text{Y}, \text{Yb}, \text{Er}, \text{Tm}$ ) [1] or YBCO/Ag composites [2]. Recently, new methodologies based on surface melting have been developed, leading to high quality welds [3],[4]. In these processes, the interface crystallizes epitaxially under a slow cooling process with respect to the adjacent YBCO blocks, which serve as “seeds” for the weld growth.

The need to evaluate the quality of the superconducting

joins has stimulated the development of different experimental characterization methods, e.g. direct transport current measurements [5], inductive measurements in ring-shaped samples containing joints [6], magnetoresistance [7], levitation force technique [8], magneto-optical imaging [8] and Hall probe mapping magnetometry [4]. The last two techniques allow visualizing how the magnetization is distributed over the surface of the sample in the remanent state. Until now, magnetization mapping of the sample under applied fields was only possible with magneto-optics, though only in the very low field range ( $<0.2$  T), because of the magnetic saturation of the ferromagnetic granate. We have developed an in-field Hall probe magnetic mapping system that allows measuring the local magnetization both in the remanence and under external fields in the  $-1$  to  $1$  T range, the upper limit being limited only by the excitation magnet. This capability can provide very useful information on the dynamics of the magnetization, and its correlation with the microstructure and defects of the sample. In addition to the local information, the magnetization over the whole sample can be integrated to obtain the global sample magnetization hysteresis cycle. Finally, the distribution of currents through the sample can be determined from the Hall magnetization maps. We used the Caragol software package to solve the inverse problem, and obtain current distribution maps at different points along the magnetization vs. applied field cycle. This method allows us to determine the distribution and magnitude of the local currents all over the sample, in particular at the joining.

In this paper we demonstrate the potential of the in-field Hall probe mapping system developed to characterize artificial welds prepared by our new silver-induced surface melting technique.

## II. EXPERIMENTAL

Single domain YBCO monoliths were prepared by the Top Seeding Growth technique, following previously developed processes [9],[10]. Table I resumes the characteristics of the samples considered. Parallelepipedic samples were extracted, and cut perpendicular to the ab plane into two pieces. The two surfaces were re-joined with a silver interface. The welding thermal treatment consisted essentially of an overheating at a temperature slightly below the peritectic temperature of YBCO and above the Ag melting point, followed by a slow

Manuscript received August 6, 2002. This work was supported in part by the European Commission under Grant RTN1-1999-00282, “Supermachines”.

S. Iliescu, S. Sena, E. Bartolomé, X. Granados, T. Puig and X. Obradors are with the Institut de Ciència de Materials de Barcelona, Campus UAB, 08193 Bellaterra, Spain, (phone 34-93-580-18-53, fax 34-93-580-57-29, e-mail: ebartolome@icmab.es).

M. Carrera is with the Dept. Medi Ambient i Ciències del Sòl, Universitat de Lleida, Jaume II, 69. 25001 Lleida, Spain.

J. Amorós is with the Dept. Matemàtica Aplicada I, Universitat Politècnica de Catalunya, Diagonal 647, Barcelona, Spain.

S.Krakunovska and T. Habisreuther are with IPHT, Winzerlaer Str. 10, Jena, D-07745, Germany

TABLE I  
OVERVIEW SAMPLES STUDIED

Sample	Source	Dimensions a x b x c (mm)	Welding process
A	ICMAB	5.65 x 5.23 x 4.92	Ag welding
B	IPHT-Jena	3.77 x 2.15 x 4.86	Ag welding
C	IPHT-Jena	5.64 x 3.96 x 2.29	Loctite glueing

Composition samples made at: ICMAB: 69%wt.  $\text{YBa}_2\text{Cu}_3\text{O}_7$ , 30%wt.  $\text{Y}_2\text{BaCuO}_7$ , 1%wt.  $\text{CeO}_2$ ; Jena:  $\text{Y}_{1.5}\text{Ba}_2\text{Cu}_2\text{O}_{7-x}$ , 1%  $\text{CeO}_2$ .

cooling process within a temperature window  $T_1$ - $T_2$ . A reoxygenation process was applied to recover the superconductivity of the sample. This technique provided good quality welds, as evidenced from the SEM-EDX and magnetoresistance measurements performed, reported elsewhere [11].

The developed Hall mapping system consists basically of a AsGa Hall probe with an active area of  $0.1 \times 0.1 \text{ mm}^2$ , that sweeps the sample surface at a flying distance of  $80 \mu\text{m}$ , in steps of  $dx=dy=160 \mu\text{m}$  (at best  $20 \mu\text{m}$ ). The system field noise was measured to be smaller than  $4 \times 10^{-5} \text{ T}$  (at  $2 \times 10^{-3} \text{ Hz}$ ). The Hall system is located in a dewar placed between the two poles of an electromagnet, which allows applying an homogeneous magnetic field  $H$  perpendicular to the sample surface, ranging from  $-1$  to  $1 \text{ T}$  [12]. The local magnetization is obtained by subtracting the applied field from the local magnetic induction  $B_z(x,y)$  measured over the surface:  $M_{\text{Hall}}(x,y) = B_z(x,y) - H$ . The global magnetization  $M$  is obtained by integration of  $M_{\text{Hall}}(x,y)$  over the sample. One can either follow a field-cooled (fc) process under the maximum available field, in order to determine the remanent magnetization; or apply a zero-field-cooled (zfc) process and measure successive maps at different applied fields.

### III. RESULTS AND DISCUSSION

Hall magnetization measurements were performed before and after the welding process, in order to control the quality of the original single domains, and be able to compare the images of the unwelded and welded samples. The simplest test available with the Hall system is the remanent magnetization map of the sample after following a fc process.

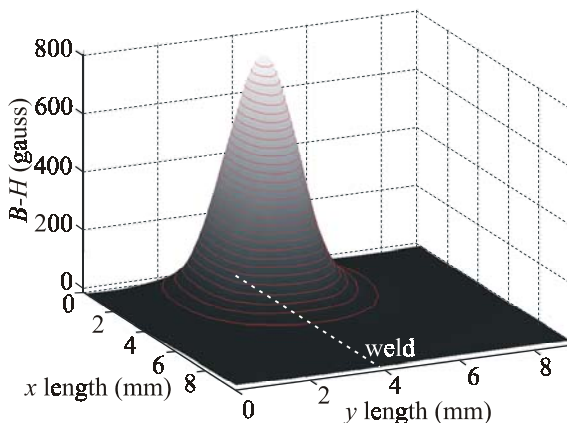


Fig.1. Hall probe remanent magnetization map after a fc process of the ab

plane of a good quality weld (A).

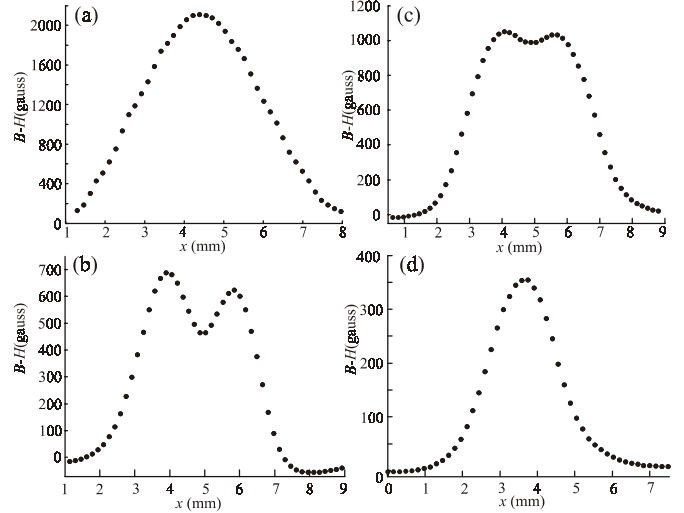


Fig. 2. Section perpendicular to the weld of the fc remanent magnetization for (a) original monocrystal (B); b) glued sample (C); (c) welded sample (B); (d) welded sample (A). Note that the absolute remanent magnetization of the samples is not comparable since the sample dimensions were different.

A section of the remanent magnetization for a single domain (Fig. 2a) presents typically a single peak, corresponding to the trapping of flux at the center of the sample. The decrease in the remanent magnetization along the weld has been used before [4] as a criterium to separate bad quality joints from good ones. We were able to obtain very high quality welds using our new Ag welding technique. Indeed, we can observe from the 3D plot of Fig. 1 that the remanent magnetization over a typical well-joined sample shows a single penetration field pattern. For comparison purposes, we report on Fig. 2 the remanent magnetization across the weld of (b) a completely non-superconducting join, achieved by simply gluing together two YBCO single domains, showing two clearly differentiated peaks; and (c) a medium quality weld, showing two less pronounced peaks, resulting from partial entry of flux at the joint. We note that in our system the distance between the Hall probe raster and the sample surface is very small ( $80 \mu\text{m}$ ) compared with other Hall systems ( $\sim 0.5 \text{ mm}$ ), so the double peak pattern of bad quality joints can be well resolved.

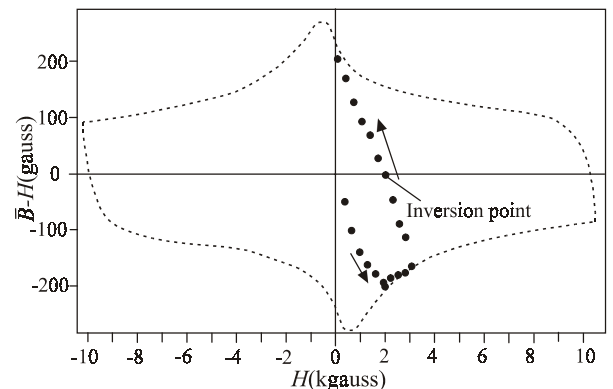


Fig. 3. Typical hysteretic magnetization vs. applied field cycle (line) and example of a of minor loop measured after a zfc process (sample B).

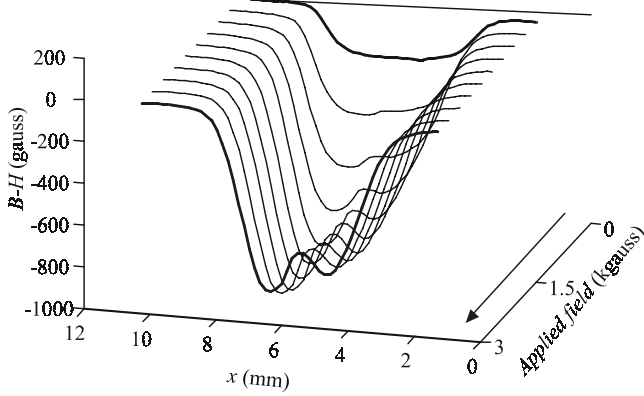


Fig. 4. Cross-section of the magnetization after a zfc process for different applied fields increasing from 0 to 3 kgauss, for the medium quality weld (B).

We investigated further the welds by measuring after a zfc process the magnetization maps at different applied fields. This procedure allows obtaining the global hysteretic magnetization  $M(H)$  cycles of the samples (Fig. 3), which can be directly compared with the cycles measured e.g. with SQUID magnetometry [12]. Fig 4. shows the magnetization measured after a zfc process as the applied field increases from 0 to 3 kgauss for a medium quality weld. We can observe that a double peak develops at high fields, evidencing that the current density across the weld is smaller than the overall current, and has a stronger field-dependence, as expected. This double peak behavior is not observed in the good quality weld, even at 3 kgauss. The advantage of the in-field measurements to evaluate the quality of the welds is thus demonstrated.

It is particularly interesting to observe the dynamic process of inversion of the magnetization over the cross point  $M=0$ . The inversion processes measured (Fig. 5, left) for a single domain, medium quality, and good quality welds can be qualitatively well described with the Bean critical state model schemes (Fig. 5, right). In a single domain sample, for a certain applied field  $H < 2H_p$ , shielding currents circulate all over the sample in one direction, producing a single non-null magnetization peak. As the field  $H$  is brought to the  $H(M=0)$  inversion point, the sample outermost currents change sign with respect to the central currents. Thus, the magnetization section shows a central  $M < 0$  peak and two adjacent  $M > 0$  peaks, as can be seen in Fig. 5a. In a medium quality weld, for an applied field  $H < 2H_p$ , the two intragrain currents at the two joined single-domains, and the weaker intergrain current, running over the whole sample, circulate in the same direction, and two non-null magnetization peaks are observed. The inversion happens when at  $H(M=0)$  the external intergrain current circulates opposed to the direction of the two intragrain currents. Two  $M < 0$  peaks at either grain and three compensating  $M > 0$  peaks can be observed (Fig. 5b). In a good quality weld, a single magnetization peak at applied field  $H$  is observed, implying that the magnitude of the intra- and inter-

grain currents are comparable. However, since it is practically impossible to have two identical joined grains, the inversion process is asymmetric, not as canonical as for the single

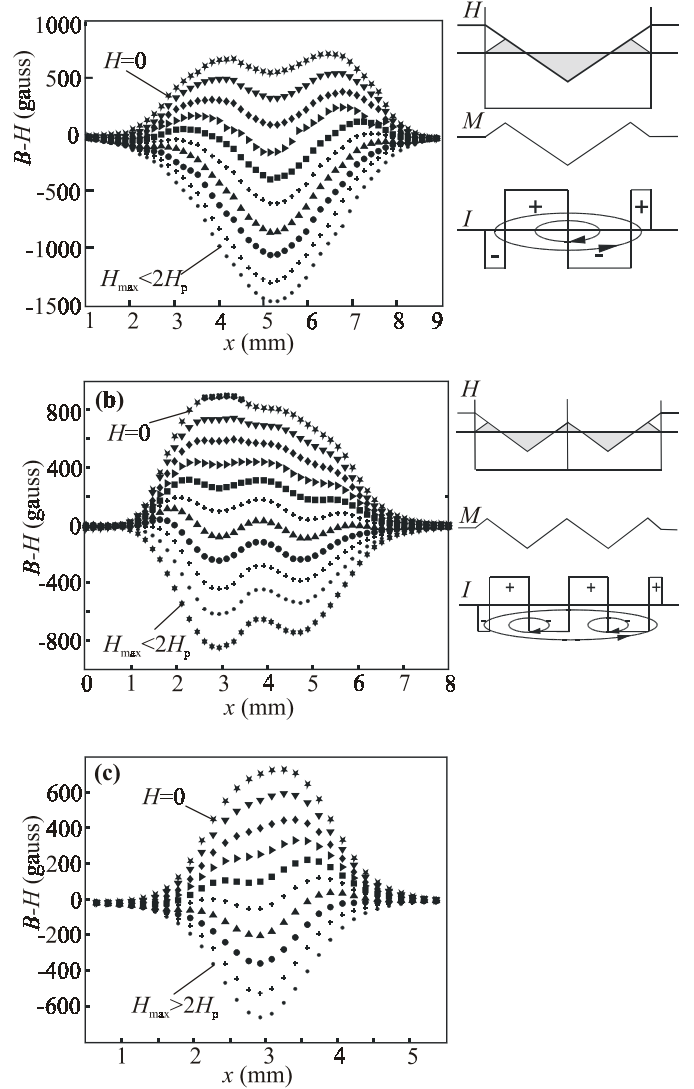


Fig.5. Left: Magnetization after a zfc process for different applied fields (going from  $H=3$  kG-0 kG-3kG in 10 steps) around the inversion point ( $M=0$ ) for (a) a single domain (B), (b) a medium quality weld (B) and (c) a good quality weld (A). Right: Bean model schematics for the applied field, magnetization and current at the inversion point (see text).

domain case (Fig. 5c). Notice that in this case the maximum applied field  $H_{max}$  was larger than  $2H_p$ , and thus the magnetization was fully reversed at  $H=0$ , in contrast to the example shown in Fig. 5a.

In order to have quantitative information about the distribution of currents over the sample, and the absolute magnitude of the critical current, the current maps associated to the magnetization maps were computed using the software package Caragol [13]. The program basically solves the inverse Biot-Savart problem in a “quasi” 3-D mode, i.e. the current density circulation  $j_c$  is considered to be planar and uniform along the sample thickness ( $z$ -axis), but no assumptions on the contour of the sample are taken. The

calculated current distribution of a good quality weld in the remanence (Fig. 6) shows a single circulation loop over the whole sample, and is indistinguishable from that of an

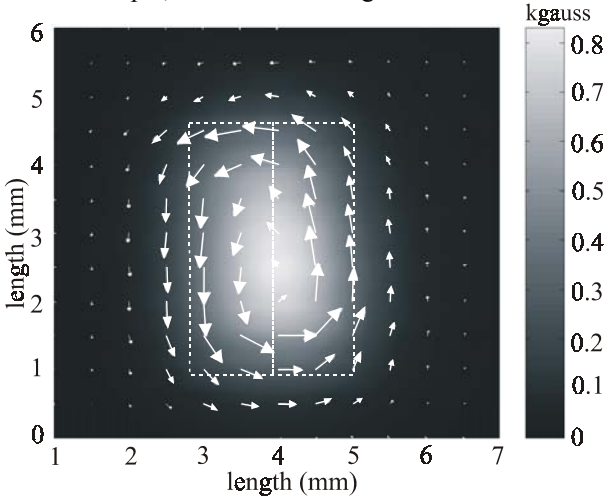


Fig. 6. Calculated current distribution superposed with the Hall magnetization map in the remanence after a fc process of a good quality weld (A). The position of the weld and sample limits are indicated for clarity.

unwelded sample. The value of the critical current obtained,  $J_c = 1.2 \times 10^9$  A/m<sup>2</sup> is typical of good quality melt-textured YBCO crystals. This confirms the success of our new technique to produce high critical current welds. In contrast, the current distribution of a medium quality weld (Fig. 7a) presents an intergrain current  $J_c^{GB}$ , and two intragrain current  $J_c^G$  circulation loops at the grains, as expected from the critical state model. From the modulus of the critical current over the weld shown in Fig. 7b, approximate values for the intragrain ( $J_c^G \approx 1.2 \times 10^8$  A/m<sup>2</sup>) and intergrain ( $J_c^{GB} \approx 0.9 \times 10^8$  A/m<sup>2</sup>) critical current densities were estimated. Thus, even in the medium quality joints prepared, a ratio  $J_c^{GB}/J_c^G \sim 75\%$  was achieved.

#### IV. CONCLUSIONS

The versatility of a new developed in-field Hall probe magnetic system for the characterization of artificial YBCO joins has been demonstrated. The local and global magnetization of the sample at different applied fields have been directly measured, and the critical current distribution calculated back with the help of a Caragol software. We have shown that high quality welds could be obtained using a new Ag surface melting induced welding technique.

#### REFERENCES

[1] K. Salama, V. Selvamanickan, "Joining of high current bulk YBaCuO superconductors", *Appl. Phys. Lett.*, vol. 60, pp.898-900, 1992.  
 [2] W. Lo, D.A. Cardwell, A.D. Bradley, R.A. Doyle, Y.H. Shi, S. Lloyd, "Development of non-weak link bulk YBCO Grain boundaries for high magnetic field engineering applications", *IEEE Trans. Appl. Supercond.*, vol. 9, pp.2042-2045, 1999.  
 [3] T. Puig *et al.*, "Self-seeded YBCO welding induced by Ag additives", *Physica C*, vol.363, p.75-79, 2001.

[4] L. Chen, H. Claus, A.P. Paulikas, H. Zheng and B.W. Veal, "Joining of melt-textured YBCO: a direct contact method", *Supercond. Sci. Technol.*, vol.15, pp.1-3, 2002.

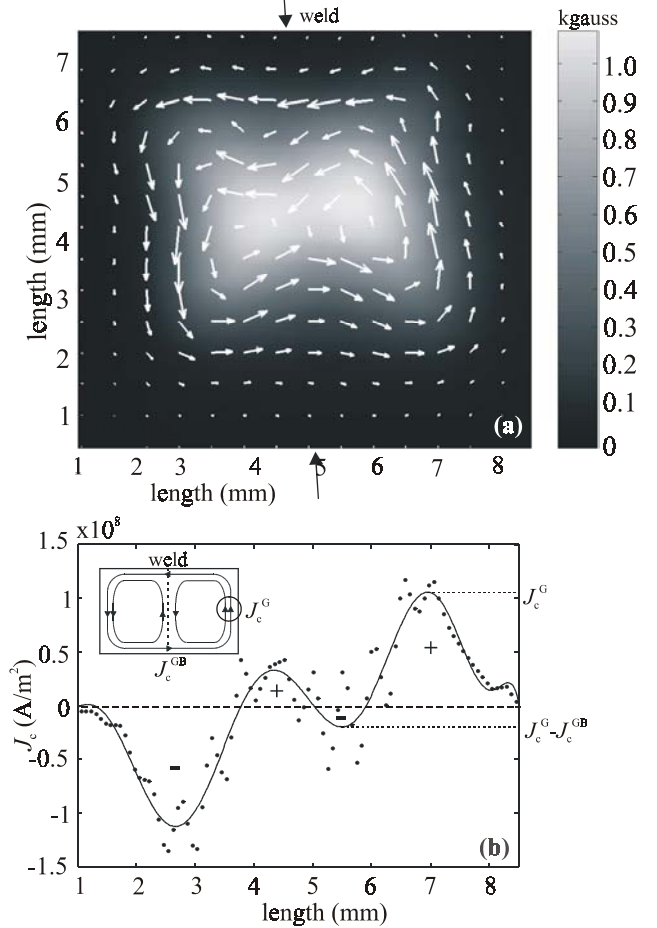


Fig. 7. Current distribution and Hall magnetization map (ab plane) in the remanence of a medium quality weld (B); (b) modulus of the critical current across the weld. The line is a guide for the eye.

[5] Ph. Vanderbemden *et al.*, "Superconducting properties of natural and artificial grain boundaries in bulk melt-textured YBCO", *Physica C*, vol.302, pp.257-270, 1998.  
 [6] B.V. Veal, H. Claus, L. Chen and A.P. Paulikas, "Studies of grain boundaries in melt-textured YBa<sub>2</sub>Cu<sub>3</sub>O<sub>x</sub>", presented at the Ceramic Society Meeting, April 2002, paper AMF 4C06.  
 [7] R.A. Doyle, A.D. Bradley, W. Lo, D.A. Cardwell, A.M. Campbell, Ph. Vanderbemden and R. Cloos, "High field behavior of artificially engineered boundaries in melt-processed YBa<sub>2</sub>Cu<sub>3</sub>O<sub>7-d</sub>", *Appl. Phys. Lett.*, vol.73, pp.117-119, 1998.  
 [8] H. Zheng *et al.*, "High critical current "weld" joins in textured YBa<sub>2</sub>Cu<sub>3</sub>O<sub>x</sub>", *Physica C*, vol.322, pp.1-8, 1999.  
 [9] X. Obradors *et al.*, "Directional solidification of ReBaCuO (Re=Y, Nd): microstructure and superconducting properties", *Supercond. Sci. Technol.*, vol.10, pp.884-890, 1997.  
 [10] T. Habisreuther *et al.*, "Requirements on melt-textured Y-Ba-Cu-O for the use in magnetic bearings or electrical rotors", *IEEE. Trans. Appl. Supercond.*, vol.11, pp.3501-3504, 2001.  
 [11] S. Ilescu *et al.*, "High quality welding of YBCO superconductors by silver induced surface melting", *unpublished*.  
 [12] X. Granados *et al.*, "Characterization of superconducting rings using an in-field Hall probe magnetic mapping system", presented in this conference.  
 [13] J. Amorós, M. Carrera, X. Granados, J. Fontcuberta, X. Obradors, "Computation of critical current through magnetic flux profile measurements", *proceedings of the European Conference on Applied Superconductivity*, Enschede, The Netherlands, 1997.